Applied Mathematics and Computation 420 (2022) 126871

Contents lists available at ScienceDirect

Applied Mathematics and Computation

journal homepage: www.elsevier.com/locate/amc

Long memory estimation in a non-Gaussian bivariate process☆

Ledys Llasmin Salazar Gomez[b], Soledad Torres[c], Jozef Kiseľák[d,e], Felix Fuders[f], Naoyuki Ishimura[g], Yasukazu Yoshizawa[h], Milan Stehlík[a,d,i,j,*]

[a] Department of Statistics, Universidad de Valparaíso, Chile
[b] Universidad Autónoma de Chile, Facultad de Administración y Negocios, Chile
[c] CIMFAV, Facultad de Ingeniería, Universidad de Valparaíso, Chile
[d] Linz Institute of Technology, Johannes Kepler University Linz, Austria
[e] P.J.Šafárik University in Košice, Slovakia
[f] Economics Institute, Universidad Austral de Chile, Independencia 631, Valdivia, Chile
[g] Faculty of Commerce, Chuo University, Hachioji, Tokyo, Japan
[h] Department of Accounting and Finance, Toyo University, Tokyo, Japan.
[i] Department of Applied Statistics, Johannes Kepler University Linz, Austria
[j] Facultad de Ingeniería, Universidad Andrés Bello, Valparaíso, Chile

ARTICLE INFO

Article history:
Received 2 February 2021
Revised 10 December 2021
Accepted 12 December 2021
Available online 30 December 2021

Keywords:
Non-Gaussian process
Student t distribution
Copula function
Hurst parameter
Discrete wavelet transform
GTCLM model

ABSTRACT

The main objective of this paper is to analyze fluctuations of foreign currency exchange rates and to identify / describe the dependence structure in stochastic processes associated with the foreign exchange market . Specifically, the study focuses on the dependence relationship between two currencies and the stochastic process underlying them. A general novel methodology is introduced, and shown to work satisfactorily on a variety of problems analyzing the bivariate financial time series possibly possessing heavy tails. This methodology can be used as powerful tool to improve the prediction of exchange rate fluctuations, which is key decision taking in monetary and fiscal policy. In the wider spectrum it can help to predict financial crises. The results could also serve to explain why the *Purchasing Power Parity* theory does not always hold.

1. Introduction

Prices of foreign currencies fluctuate on the international foreign exchange market (FX market). Such currency price fluctuations have a significant impact on the respective economies as they affect trade relations (Terms of Trade) between countries. This impact is twofold. Since prices of imported products vary depending on the exchange rate, so does the purchasing power of households. Also, macroeconomic variables as exportation and gross domestic product and Inflation are strongly depended on exchange rates. For example, the appreciation of a country's currency will, everything else being equal, slow down exportations and reduce the costs of imports and hence decrease inflation (so-called exchange rate pass-

☆ Fully documented templates are available in the elsarticle package on CTAN.

* Corresponding author at: Department of Applied Statistics, Johannes Kepler University Linz, Austria.
E-mail addresses: ledys.salazar@cloud.uautonoma.cl (L.L.S. Gomez), soledad.torres@uv.cl (S. Torres), jozef.kiselak@upjs.sk (J. Kiseľák), felix.fuders@uach.cl (F. Fuders), naoyuki@tamacc.chuo-u.ac.jp (N. Ishimura), Milan.Stehlik@jku.at (M. Stehlík).

https://doi.org/10.1016/j.amc.2021.126871

through, see e.g. [11]). To be able to predict these fluctuations, is key for estimating exportation, gross domestic product and inflation and, thus, for decision taking in monetary and fiscal policy, and in the wider spectrum it can even help to predict financial crises. Stochasticity in finance can be well supported in the recent studies. Finance and economics are complex nonlinear systems, affected by various external factors and several important contributions have been made recently, e.g. see [33] for study of the dynamics and complexity in a fractional-order financial system with time delays. Sigaki et al. [6] uses permutation entropy and statistical complexity over sliding time-windows of price log returns to quantify the dynamic efficiency of more than four hundred cryptocurrencies.

The main objective of this paper is to analyze price fluctuations between currencies and to identify / describe the dependence structure in stochastic processes associated with the foreign exchange market and, in so doing, to contribute to more accurately being able to predict price fluctuations of exchange rates. Specifically, we focus on the dependence relationship between two currencies and the stochastic process underlying them. We will introduce a general novel methodology, called the GTCL, which has shown to work satisfactorily on a variety of problems analyzing the bivariate financial time series possibly possessing heavy tails. It is well known that the time series of returns in finance do not always follow a Gaussian copula and some see in this the reason for the financial meltdown at Wall Street in 2008 [13,17], since so-called 'David Li's formula' [21] was based on just this idea. Here we give not only ideas for why the returns do not follow a Gaussian distribution but, also, new insights that could explain of why the so-called Purchasing Power Parity theory, according to which the same amount of any currency could buy the same basket of products everywhere [9,22], does not always hold. Usually, the exchange rate of a currency against another currency is seen to depend on variables such as gross domestic product or Consumer Price Index (e.g, [9]). However, the relation only indirectly is correlated with gross domestic product or inflation or other parameters of each country. As any market, the foreign exchange markets are driven by supply and demand, here the supply and demand of a certain currency, while its price is measured in another currency. As any good is measured in units of the respective country's currency, in the foreign exchange markets the 'good' traded is the foreign currency; and its price is expressed in the currency of the country in which the foreign exchange market is established. For example, in the US all foreign currencies are traded in USD. The foreign exchange market in Japan prices other currencies in JPY. The foreign exchange market in Switzerland expresses prices of other currencies in CHF, and so on. In the following Section 3 we will examine the JPY/CHF exchange rate.

2. Methodology

We will start defining the returns of an investment in each currency and the joint behavior through the construction of the 2-dimensional copula. Next, we analyze the memory. The initial phase allows to visualize the distribution of the returns, which do not always follow a Gaussian distribution; in addition, the 2-dimensional copula illustrates a behavior of extreme value copulas, specifically the Student t. This is why we dedicate part of this study to the analysis of the distributional assumption of the data. In this sense, we require the use of some technique that allows the estimation of the parameters. In this regard [8,27,28] provide tools in this context. For financial returns that show a non-Gaussian behavior, particularly a Student t behavior, Sánchez Ovando [27] yields the possibility of change the random variable Student t into a random Gaussian variable by multiplying the Student t by an inverse gamma. According to this idea we establish an initial approximation to data. The multivariate Gaussian distribution assures that each of the marginal is Gaussian; and if the covariances are zero then random variables are independent. In our case all covariances are significantly different from zero, that is, there exists dependence between the variables. Moreover, we analyzed the memory by estimation of Hurst parameter H which quantifies the memory of the process (see [3,30,32]). Once we transformed our data to the Gaussian vector, we estimate 55 the value of H_1 and H_2 for each of its marginal. In the recent literature, several methods have been developed for testing of H, e.g., generalized quadratic variation, wavelet coefficients, aggregate variance, re-scaled range, discrete wavelet transform, among others (see [1,3,15,18] among others). Here we used the discrete wavelet transform for the H estimation. Having the bivariate copula and the values of H_1 and H_2 at hand, we can adequately study the underlying stochastic process of the financial series. The manuscript is organized as follows. In the following Section 3 we provide the estimation of the parameters of the Student t distribution along with the coefficient of tails and some measures of dependence. Moreover, we develop the methodology for transforming a random Student t variable into a Gaussian variable and we provide the memory of a fractional Brownian motion (FBM), we construct the discrete wavelet transform and the coherence function between two fractional Brownian motions. Sections 4 and 3.3 expose the construction of the generalized TCLM model. In Section 6 the analysis of the data is presented. Finally, Section 7 presents some comments and conclusions.

3. Preliminaries

3.1. Non-Gaussian bivariate process

It is known in the financial area that the time series of some returns do not always follow a Gaussian distribution. One can find returns that follow distributions with heavy tails, e.g. Student t. For instance, the frequency for the returns of CHFJPY and EUROJPY currencies of the Japanese bank (see Figs. 1 and 2), together with the normality tests for each of the series, provided the evidence that these returns do not follow a Gaussian distribution.

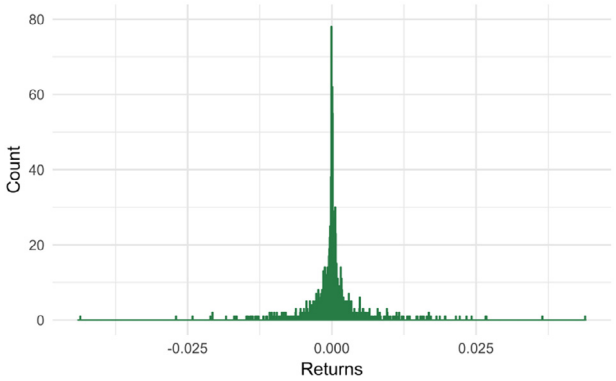

Fig. 1. Heavy tailed distribution of returns of the CHFJPY implying non-Gaussianity.

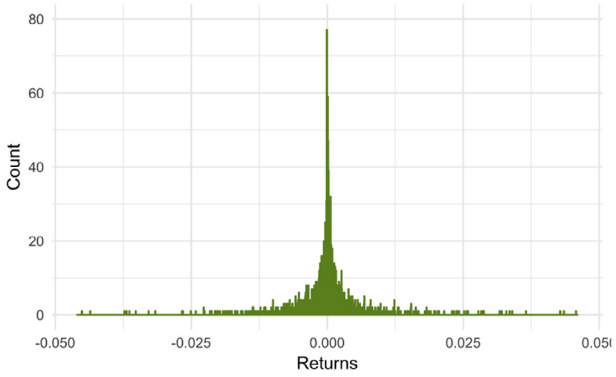

Fig. 2. Heavy tailed distribution of returns of the EUROJPY implying non-Gaussianity.

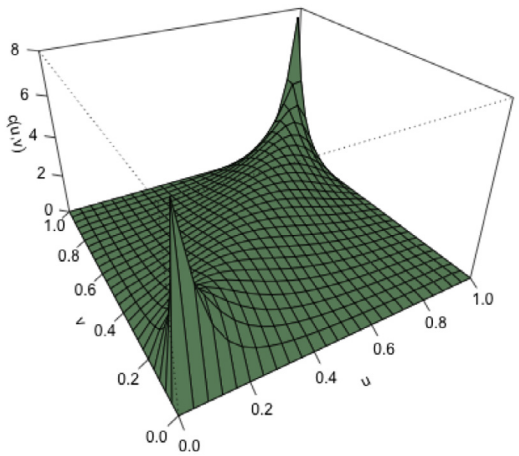

Fig. 3. Joint probability density function of Student t copula for bivariate modeling of pair currencies CHFJPY and EUROJPY.

This motivates the study of non-Gaussian returns and the study of their theoretical and practical implications. In order to recognize the distributional character of the data (returns of currencies) we need to understand the characteristics of the stochastic process underlying the time series. Figs. 1 and 2 show the marginal behavior of the series, but what happens with the joint behavior (the bivariate stochastic process that involves both currencies)? If we construct the 2-dimensional copula with these marginals, we obtain the bivariate Student t distribution as shown in Fig. 3.

In the next subsection we will provide the process of construction of the 2-dimensional copula; the degrees of freedom estimation of the bivariate process using the coefficient of tails and the correlation coefficient; and the transformation of the bivariate Student t random vector into bivariate Gaussian.

3.2. Copula function

Copula models are popular in different areas such as Finance, Biomedical Sciences, Industrial Processes, Geostatistics (see e.g. [5,29,34]) among others. Under some regularity conditions, its potential lies in the possibility of convenient modeling a dependence structure between random variables. Specifically, in the financial area there is a great interest in establishing the relationship between the joint distribution function and their respective marginal distribution functions when the random variables preserve a dependence structure. In particular, for the FX market it is useful to recognize the behavior of a currency in relation to other currencies and the copula function becomes a possible tool that allows us to address this problem. According to Nelsen [23], Sklar [31] a 2-dimensional copula is a function C from $\mathbf{I}^2$ to $\mathbf{I} := [0,1]$ with the following properties:

- For every u, v in $\mathbf{I}$,

$$C(u,0) = 0 = C(0,v) \quad and \quad C(u,1) = u \quad and \quad C(1,v) = v. \tag{1}$$

- For every u_1, u_2, v_1, v_2 in $\mathbf{I}$ such that $u_1 \le u_2$ and $v_1 \le v_2$,

$$C(u_2,v_2) - C(v_2,v_1) - C(u_1,v_2) + C(u_1,v_1) \ge 0. \tag{2}$$

where $u = F(x)$ and $v = G(y)$. Now, to construct the 2-dimensional copula we use the ML method. Remember that every joint bivariate cumulative distribution function H of a random vector (X,Y) can be expressed in terms of its marginals F, G and a copula C, i.e. $H(x,y) = C(F(x), G(y))$. Now

$$c(F(x),G(y)) = \frac{\partial^2 (C(F(x),G(y)))}{\partial F(x) \partial G(y)} \tag{3}$$

is the second partial derivative of the copula C and c is the copula density in the case that X and Y are continuous random variables. Hence

$$h(x,y) = f(x)\, g(y)\, c(F(x),G(y)) \tag{4}$$

is the density for H. For better illustration we give here next example in which we know the transition distribution, i.e. a copula, which is quite rare in praxis.

Example 1. Here we consider the bivariate Lomax distribution (Durling Pareto distribution), see [4]. It is a heavy-tail probability distribution used in business, economics, actuarial science or queuing theory. Its joint survival function is for $0 \le \beta \le (c+1)ab,\ a,b,c > 0$ given by

$$\overline{H}(x,y) = (1 + ax + by + \beta xy)^{-c},\ x \ge 0, y \ge 0.$$

It has Lomax (Pareto of the second kind) marginals $X \sim \text{Lomax}(c, 1/a),\ Y \sim \text{Lomax}(c, 1/b)$, where the cumulative distribution function of Lomax(α, λ) is $1 - \left[1 + \frac{x}{\lambda}\right]^{-\alpha}, x \ge 0$. Clearly, a and b are marginal scale parameters while β and c are dependence parameters. Moreover, it is known that X, Y are right tail increasing if $\beta \le ab$ and right tail decreasing if $\beta \ge ab$. For cumulative distribution functions $F(x), G(y)$ of X, Y respectively we have that

$$H(x,y) = \overline{H}(x,y) - 1 + F(x) + G(y),\ x,y \ge 0$$

equals $C(F(x),G(y))$ with the Lomax copula (notice that in Balakrishnan and Lai [4] there is a typo in exponent in the denominator - there is $1/c$ instead of c)

$$C(u,v) = \frac{(1-u)(1-v)}{\left(1 - \left(1 - \frac{\beta}{ab}\right)\left[1 - (1-u)^{\frac{1}{c}}\right]\left[1 - (1-v)^{\frac{1}{c}}\right]\right)^c} + u + v - 1 \tag{5}$$

If $\beta = 0$, then associated survival copula $\hat{C}$ is known as Clayton copula (also as Pareto copula). The case $\beta = ab$ corresponds to the independence case (also for $c \to \infty$) and $c = 1$ is nothing but the Ali–Mikhail–Haq family of an Archimedean copulas. Here we have $G_{Y|X=x}(y) = 1 + \frac{\overline{H}(x,y) - \overline{F}(x)}{\overline{G}(y)}$.

Let $\boldsymbol{\theta} \in \Theta$ be the parameter vector to be estimated. This parameter vector can be split up (see [12]) into the parameters for the marginals and the copula function as follows $\boldsymbol{\theta} = [\xi, \gamma, \delta]^T$.

Here $\xi \in \Xi$ denotes the estimated parameters of the density function $f(x)$ that maximize the likelihood function over the parametric space Ξ. $\gamma \in \Gamma$ denotes the estimated parameters of the density function $g(y)$ that maximize the likelihood function within the parametric space Γ. And finally $\delta \in \Delta$ denotes the estimated parameters of the copula density $c(F(x),G(y))$ that maximize the likelihood function over parameter space Δ. Assume we observe a sample x_t and y_t for $t = 1, \ldots, T$. The representation in (4) and the resulting log-likelihood function are

$$l(\boldsymbol{\theta}) = \sum_{t=1}^{T} \ln f(x_t;\xi) + \sum_{t=1}^{T} \ln g(y_t;\gamma) + \sum_{t=1}^{T} \ln(c(F(x_t;\xi), G(y_t;\gamma));\delta), \tag{6}$$

where

$$\hat{\boldsymbol{\theta}}_{MLE} = \underset{\boldsymbol{\theta}\in\Theta}{\operatorname{argmax}}\, l(\boldsymbol{\theta}).$$

This estimator is efficient under regularity conditions when the amount of data available for the two series is equal. However, it may be computationally difficult to obtain these estimates (see [12]).

Once the copula and its respective parameters are estimated, we can estimate Kendall's τ, Spearman's ρ coefficients jointly with the tail dependence parameter λ. According to [8,14] these values allow us to calculate $\hat{\nu}$ for the bivariate process using the expression

$$\lambda = \frac{\int_r^{\frac{\pi}{2}} \cos^{\nu} t\, \mathrm{d}t}{\int_0^{\frac{\pi}{2}} \cos^{\nu} t\, \mathrm{d}t}, \tag{7}$$

for the 2-dimensional Student t, $r = (\frac{\pi}{2} - \arcsin\rho)/2$, ν is tail index of the distribution. Note that this quotient can be expressed using the Gaussian hypergeometric function ${}_2F_1(a,b;c;z) = \sum_{n=0}^{\infty} \frac{(a)_n (b)_n}{(c)_n} \frac{z^n}{n!}$. Indeed, for $\nu > -1$ we have

$$\int_r^{\frac{\pi}{2}} \cos^{\nu} t\, \mathrm{d}t = \frac{\cos(r)^{1+\nu}\, {}_2F_1(1/2, (1+\nu)/2;\ (3+\nu)/2;\ \cos(r)^2)}{1+\nu},\ r \in [0, \pi/2],$$

which for $r = 0$ yields $\frac{\sqrt{\pi}\,\Gamma((3+\nu)/2)}{(1+\nu)\,\Gamma(1+\nu/2)}$. This gave us an estimator of degrees of freedom $\hat{\nu}$ of the bivariate process, i.e. initially we used the ML method to estimate the parameters of the copula, and next, we determined $\hat{\nu}$ using the coefficients ρ and λ. It is very important to clarify that the procedure used to determine $\hat{\nu}$ in the bivariate process with both currencies is completely different from the procedure used to estimate the marginal degrees of freedom. To know $\hat{\nu}$ is useful for the application of some basic theorems. For example, [8] illustrates the possibility of transforming the Student t random variable into a Gaussian by knowing in advance the degrees of freedom of the Student t. According to [8], a Student t random variable $X \sim t(\nu, 0, \sigma^2)$ can be transformed into a random Gaussian variable by weighing it with an inverse gamma, i.e. in a bivariate case for random vectors we have

$$W^{-1}\mathbf{X} = \mathbf{Z}, \tag{8}$$

where $\mathbf{X} \sim t_2(\nu, 0, \Sigma)$, where $\mathbf{Z} \sim N(0, \Sigma)$, W is independent of $\mathbf{Z}$ and $W \sim Gamma(\nu/2, \nu/2)$.

Thereby, calculating $\hat{\nu}$ from a Student t distribution allows us to obtain a Gaussian distribution by applying (8). In a multivariate Gaussian distribution, it is possible to secure that each of the marginal is a univariate Gaussian. In addition, if the covariances are null, the random variables are independent. In this particular study, we focus on the case where covariances are different from zero, that is, we consider the dependence between the variables. Thereby we proceed with the extraction of univariate Gaussian variables and analyze their marginal behavior. In the first place, we verified some assumptions: stationarity, self-similarity and dependence between the increments. Then we proceed with the analysis of memory by estimation of Hurst exponents H_1 and H_2.

3.3. Transformation for non student vector

One of the key ideas of the TCLM model is the transformation of the Student vector into a Gaussian one. However, similar construction can be done also for other copulas, which is a base of our model in Section 4. This can be done using the following Theorem 1.

Theorem 1. *There exists a transformation, which maps an absolutely continuous bivariate random vector into a bivariate normal vector.*

Indeed, we know that random vector $R = (X, Y)$ can be expressed in terms of its marginals F, G and a copula C. Thus we might suppose that it is given by the distribution function $H(x, y) = C(F(x), G(y))$. Now, we set on the R the transformation T as follows, see [26],

$$T: \quad u = P[X \le x] = F(x), \quad v = P[Y \le y | X = x] = G_{Y|X=x}(y).$$

Then for $TR = (U, V) =: J$ we have $P[U \le u] = P[X \le x] = u,\ u \in \mathbf{I}$ (zero otherwise) and (again for $(u, v) \notin \mathbf{I}^2$ it is clearly zero)

$$P[U \le u, V \le v] = \int_0^u \int_0^v \mathrm{d}F_{U,V}(\tilde{u}, \tilde{v}) = \iint_{\{J: U \le u, V \le v\}} \mathrm{d}G_{Y|X=x}(y)\, \mathrm{d}F(x)$$

$$= \iint_{[0,u]\times[0,v]} \mathrm{d}\tilde{u}\, \mathrm{d}\tilde{v} = uv,\ (u, v) \in \mathbf{I}^2.$$

This means that $J \sim U(\mathbf{I}^2)$ (uniformly distributed on unit square) and that U, V are independent. Now, if the cumulative distribution function of the standard normal distribution is the integral $\Phi(x) = \frac{1}{\sqrt{2\pi}} \int_{-\infty}^{x} e^{-t^2/2}\, dt$, then

$$\tilde{T}: \quad \tilde{U} := \Phi^{-1}(U), \quad \tilde{V} := \Phi^{-1}(V)$$

$\left(\Phi^{-1}(p) = \sqrt{2}\,\mathrm{erf}^{-1}(2p-1),\ \ p \in \mathbf{I}^{\circ}\right)$ are two independent standard normal random variables. Independence follows from the fact, that U, V are independent. Therefore $\tilde{J} = (\tilde{U}, \tilde{V}) \sim N(0, I)$ and it is well known that the affine transformation Af : $Z = \mu + A\tilde{J}$ with the matrix

$$A = \begin{pmatrix} \sigma_1 & 0 \\ \rho\,\sigma_2 & \sigma_2\sqrt{1-\rho^2} \end{pmatrix}$$

and vector $\mu = (\mu_1, \mu_2)$ we obtain that $Z \sim N(\mu, AIA^T) = N(\mu, \Sigma)$ with

$$\Sigma = \begin{pmatrix} \sigma_1^2 & \rho\,\sigma_1\sigma_2 \\ \rho\,\sigma_1\sigma_2 & \sigma_2^2 \end{pmatrix}.$$

Together we have found a mapping $Af \circ \tilde{T} \circ T$ that send random vector R to a normally distributed random vector Z.

3.4. Fractional Brownian motion

According to Shevchenko [30] a fractional Brownian motion is a centered Gaussian process $B_t^H, t \geq 0$ with the covariance function

$$E(B_t^H, B_s^H) = \frac{1}{2}\left(t^{2H} + s^{2H} - |t-s|^{2H}\right). \tag{9}$$

From the definition (9) can be deduced some properties: stationary increments, self-similarity, dependence of increments and the following holds:

$$E\left[(B_{t_1}^H - B_{s_1}^H)(B_{t_2}^H - B_{s_2}^H)\right] < 0, \text{ for H} \in (0, 1/2) \tag{10}$$

and

$$E\left[(B_{t_1}^H - B_{s_1}^H)(B_{t_2}^H - B_{s_2}^H)\right] > 0, \text{ for H} \in (1/2, 1). \tag{11}$$

Thus, for $H \in (0, 1/2)$, the fractional Brownian motion has the property of counter-persistence: if it was increasing in the past, it is more likely to decrease in the future, and vice verse. In contrast, for $H \in (1/2, 1)$, the fractional Brownian motion is persistent, it is more likely to keep trend than to break it. Moreover, for such H, the fractional Brownian motion has the property of long memory (long-range dependence), see [30]. When $H = \frac{1}{2}$ in the Eq. (9) the fractional Brownian motion is a standard Brownian motion and there the covariance between two different equidistant time periods is zero. So, H is a measure of how predictable the time series can be in terms of its trend. Since the upward or downward trend of financial returns provides useful information on the behavior of economic variables, in addition, knowing the trend allows investors to have more information for decision making. The Hurst parameter H should be estimated, however, there is a range of possibilities in literature for its estimation; e.g. [3,16,18], among others.

4. GTCLM model construction

In the context of financial time series, it is initially recommended to extract the percentage variation or returns, and then, perform the statistical analysis.

In the next steps, we propose the GTCLM model as a possible way to capture the subjacent stochastic process in the dependence relation between two currencies. Initially we check the distributional assumption of the returns of both currencies using different tests. The statistical tests justified that the two series do not reflect a Gaussian behavior. Additionally, we constructed the 2-dimensional Student t copula. Then, knowing the copula and its respective parameters, we proceed with the calculation of $\hat{\nu}$ using (7); subsequently, we apply (8) and obtain the bivariate Gaussian distribution. Remember that the bivariate Gaussian distribution ensure that each of the marginal ones is Gaussian, allowing us to proceed with the extraction of the marginals. The great utility of univariate Gaussian densities lies in the possibility of using the basic theory of stochastic processes.

Further we analyzed memory of each of the marginals. Initially we verified that the increments are stationary, self-similar and dependent; then, we estimated Hurst exponents for each of the series, $\hat{H}_1$ and $\hat{H}_2$, respectively. Using the functions $\psi_{j,k}$ as a set of filters, we used the discrete wavelet transform which consists of a decomposition time series according to the sample path of an initial series $X(t)$; a time series with the detail coefficients $(d_{j,k})$ and other with the scale coefficients $(a_{j,k})$. According to Abry et al. [1] $a_{j,k}$ and $d_{j,k}$ are defined as follows

$$a_{j,k} = \int_{-\infty}^{\infty} X(t)\phi_{j,k}(t)\,\mathrm{d}t \tag{12}$$

and

$$d_{j,k} = \int_{-\infty}^{\infty} X(t)\psi_{(j,k)}(t)\,\mathrm{d}t, \tag{13}$$

where $\phi_{j,k}(t) = 2^{-j/2}\phi(2^{-j}t-k)$, $\psi_{j,k} = 2^{-j/2}\psi(2^{-j}t-k)$, ψ is the mother wavelet defined through a scaling function ϕ and $\psi(t-k)$ is the translation of ψ to the right by k units, 2^j is the scale and $j,k \in \mathbb{Z}$. Kaplan [16] suggests to obtain $\hat{H}$ by a linear regression on the values using the expression

$$\log_2\left(\frac{1}{n_j}\sum_{k=1}^{n_j}|d_{j,k}|^2\right) \tag{14}$$

on j, where j represents the decomposition level. To calculate $\hat{H}$, Kaplan [16] uses the equation

$$\hat{H} = \left|\frac{\beta-1}{2}\right|, \tag{15}$$

where β is the slope on the regression line on (14) respect to j. Specifically, we used the above method to determine $\hat{H}_1$ and $\hat{H}_2$ in the two currencies.

Finally, we proceed with the reconstruction of the bivariate process using the obtained estimates ($\hat{\nu}$ and the covariance matrix Σ), and subsequently, with the analysis of the coherence function between the two fractional Brownian motions ($\hat{H}_1$ and $\hat{H}_2$). Here it is important to analyze what happens between the two trajectories of the process, for this, we analyze the cross-covariance between both processes. Let $X = \{X(t), t \in \mathbb{R}\}$ be a process with values in $\mathbb{R}^p$ with finite second moments. Assume that X has stationary increments, zero mean, $X(0) = 0$, and that X is vector self-similar with exponent $H = \mathrm{diag}(H_1, \ldots, H_p)$, $0 < H_i < 1$, $i = 1, \ldots, p$. Moreover, assume that for any $i, j = 1, \ldots, p$, the function $t \mapsto EX_i(t)X_j(1)$ is continuously differentiable on $\mathbf{I}^\circ \cup (1, \infty)$. Let $\sigma_i^2 > 0$ denote the variance of $X_i(1)$, $i = 1, \ldots, p$. If $i \neq j$ and $H_i + H_j \neq 1$, then there exists c_{ij}, $c_{ji} \in \mathbb{R}$ such that for any $(s,t) \in \mathbb{R}^2$

$$\mathrm{Cov}(X_i(s)X_j(t)) = \frac{\sigma_i\sigma_j}{2}\left\{c_{ij}(s)|s|^{H_i+H_j} + c_{ji}(t)|t|^{H_i+H_j} - c_{ji}(t-s)|t-s|^{H_i+H_j}\right\}, \tag{16}$$

where $c_{ij}(t) = \begin{cases} c_{ij}, & t > 0 \\ c_{ji}, & t < 0 \end{cases}$, see [19]. With respect to $c_{ij}(t)$, [19] asserts that:

$$c_{ij}(t) = 2\frac{\tilde{c}_{ij}p_{ij}}{\sigma_i\sigma_j}, \quad p_{ij} = \frac{B(H_i+0.5, H_j+0.5)}{\sin((H_i+H_j)\pi)},$$

where B is the Beta function and the matrix $\tilde{C} = (\tilde{c}_{ij})$ is given by

$$\tilde{C} = \cos(H\pi)A_+A_+^* + A_-A_-^*\cos(H\pi) - \sin(H\pi)A_+A_-^*\cos(H\pi) - \cos(H\pi)A_+A_-^*\sin(H\pi),$$

where $A_\pm$ are real $p \times p$ matrices from a double sided stochastic integral representation of $X(t)$, A^* denotes the transposed matrix, $\sin(H\pi) = \mathrm{diag}(\sin(H_1\pi), \ldots, \sin(H_p\pi))$ and $\cos(H\pi) = \mathrm{diag}(\cos(H_1\pi), \ldots, \cos(H_p\pi))$ (see again [19]).

Now, for time shift of length $|h|$ the cross-covariance of the increments of size δ of components i and j when $H_i + H_j \neq 1$ (see [2]) is given by

$$\gamma_{ij}(h,\delta) = E\Delta_\delta X_i(t)\Delta_\delta X_j(t+h) = \frac{\sigma_i\sigma_j}{2}\big(w_{ij}(h-\delta) - 2w_{ij}(h)\big) + (w_{ij}(h+\delta)), \tag{17}$$

where

$$w_{ij}(h) = (\rho_{ij} - \eta_{ij}\,\mathrm{sign}(h))|h|^{H_i+H_j}. \tag{18}$$

and $\rho_{ij} = (c_{ij}+c_{ji})/2$ and $\eta_{ij} = (c_{ij}-c_{ji})/2$. If $S_{ij}(\omega,\delta)$ is the Fouerier transform of $\gamma_{ij}(\cdot,\delta)$, then in summary, the coherence function[1] $C_{ij}(\omega,\delta) = \frac{|S_{ij}(\omega,\delta)|^2}{S_{ii}(\omega,\delta)S_{jj}(\omega,\delta)}$ (see Section 5 for relations between geometry, polarization and coherence) between the increments of size δ between the components i and j on the 2-dimensional fractional Brownian motion are at each ω in the frequency domain given by

$$C_{ij}(\omega,\delta) = \frac{\Gamma(H_i+H_j+1)^2}{\Gamma(2H_i+1)\Gamma(2H_j+1)}\frac{\rho_{ij}^2\sin(\frac{\pi}{2}(H_i+H_j)^2) + \eta_{ij}^2\cos(\frac{\pi}{2}(H_i+H_j)^2)}{\sin(\pi H_i)\sin(\pi H_j)}. \tag{19}$$

For $p = 2$, i.e., on the 2-dimensional case, and having fixed values of H_1 and H_2, the condition $C_{12} \leq 1$ means that the set of possible parameters ρ_{12} and η_{12} is inside an ellipse, i.e., it is possible to determine the maximum correlation that may exist between the increments of the studied currencies. Fig. 4 provides flow chart for the construction of GTCLM model.

[1] Quotient of the squared magnitude of the Cross-spectral density and the product of the autospectral densities.

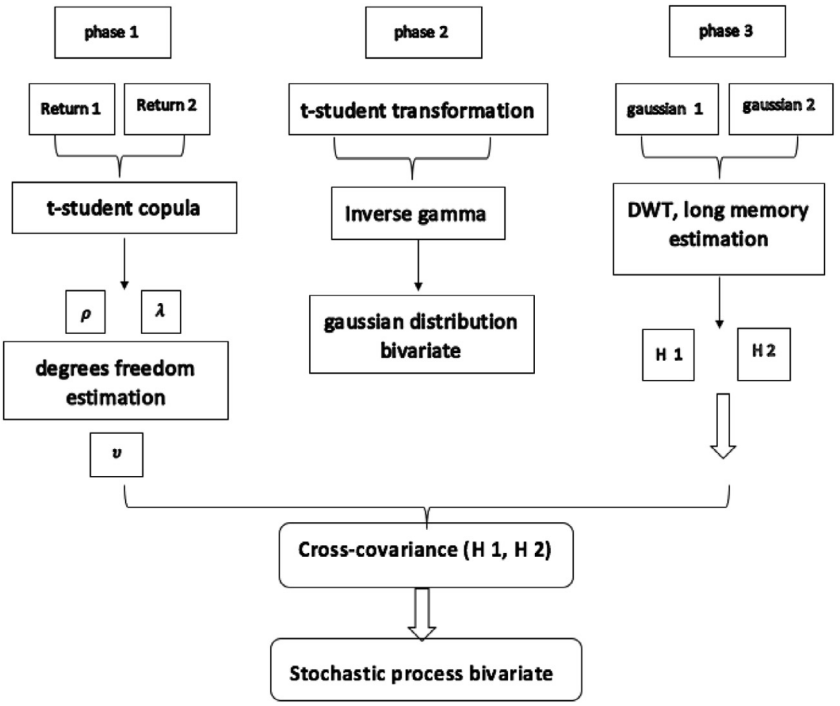

Fig. 4. Flow chart for the construction of GTCLM model.

5. Geometrical properties of bivariate case - Stokes parameters

It is observed in physical and other systems that the correlation exhibits a slower decay for large values of the delay (or distance). It may be quite important to understand the global system behavior (contrasting sharply with the exponential decay case). The particular choice of the power law as the main alternative of the exponential decay is motivated by a self-similarity of distributions. Assume a stationary random bivariate process (signal) $[x(t), y(t)]^T$ (or equivalently a complex valued random process). Its associated Stokes parameters, defined by George Gabriel Stokes in 1852, describe the polarization state at each ω in the frequency domain (originally states of electromagnetic radiation). They carry multiple information about the process. We deal with the fractional Gaussian noise[1,2,3] (FGN). It is well-known that a centered univariate Gaussian process is fully described by its autocorrelation function. To completely characterize a stationary Gaussian centered bivariate signal it is necessary to consider four second-order quantities: autocorrelation functions of x and y (S_{xx}, S_{yy}) and cross-correlation functions (S_{xy}, S_{yx}).

Stokes parameters[3] are often combined into a vector, known as the Stokes vector defined as:

$$\vec{S} = \begin{pmatrix} S_0 \\ S_1 \\ S_2 \\ S_3 \end{pmatrix} = \begin{pmatrix} I \\ Ip\cos 2\psi \cos 2\chi \\ Ip\sin 2\psi \cos 2\chi \\ Ip\sin 2\chi \end{pmatrix} = \begin{pmatrix} I \\ Q \\ U \\ V \end{pmatrix} = \begin{pmatrix} S_{xx}+S_{yy} \\ S_{xx}-S_{yy} \\ 2\,\Re(S_{xy}) \\ 2\,\Im(S_{xy}) \end{pmatrix}.$$

Here $Ip, 2\psi$ and 2χ are the spherical coordinates[4] of (S_1, S_2, S_3). The set of all polarization states are then mapped to points on the surface of the so-called Poincaré sphere, see related polarisation ellipse on Fig. 5. For Stokes vectors of the degenerate polarization states see Fig. 6. Theorem Lefèvre et al. [20, Proposition 2.1] gives us Stokes parameters for FGN. It gives direct relation between Stokes parameters auto and cross correlations and Hurst exponents. We give here a completization of this theorem. For a bivariate FGN with a pair of Hurst exponent H_1, H_2, a pair of variances σ_1, σ_2, and a

[2] A stationary centered Gaussian process described as being the increment process of the fractional Brownian motion.

[3] The quadruplet $\vec{S}$ in the frequency domain are directly related to Fourier transform pairs, i.e. $S_{xx}(\omega) = \int_{\mathbb{R}} R_{xx}(\tau)e^{-i\omega\tau}\,d\tau$, $R_{xx}(\tau) = E[x(t)x(t+\tau)]$ (autocorrelation function) and $S_{xy}(\omega) = \int_{\mathbb{R}} R_{xy}(t)e^{-i\omega t}dt, R_{xy}(\tau) = E[x(t)y(t+\tau)]$ (cross-correlation function).

[4] I is the total intensity of the beam, and p is the degree of polarization, constrained by $0 \le p \le 1$. Inverse relation is characterized as $I = S_0$, $p = \frac{\sqrt{S_1^2+S_2^2+S_3^2}}{S_0}$, $2\psi = \arctan\frac{S_2}{S_1}$, $2\chi = \arctan\frac{S_3}{\sqrt{S_1^2+S_2^2}}$.

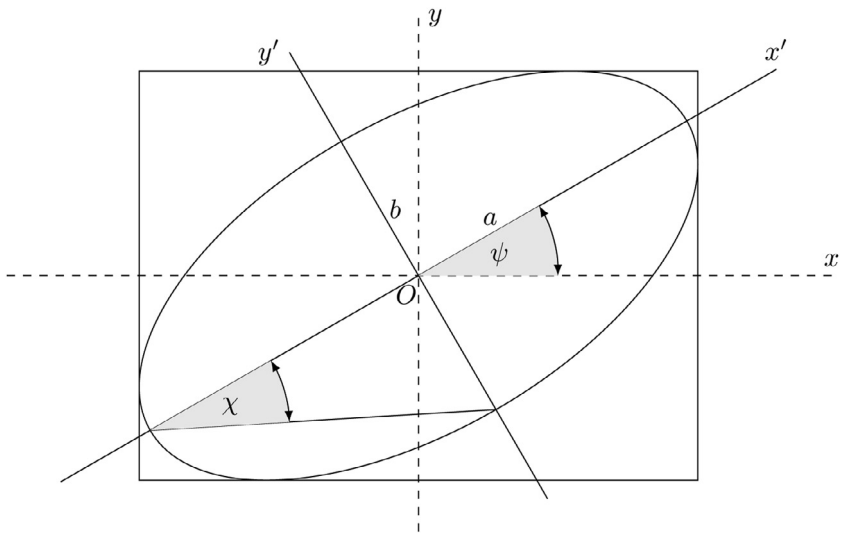

Fig. 5. Polarisation ellipse showing the orientation angle ψ and ellipticity (angle) χ, which are functions of the semi-major and semi-minor axes, a and b. The size and what is more important the shape of a two-dimensional ellipse can be defined by three parameters (e.g. by a, b and ψ).

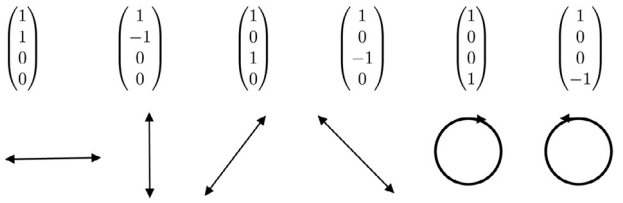

Fig. 6. Stokes vectors for the degenerate polarization states. In sequel: linearly horizontally polarized, linearly vertically polarized, linearly polarized ($+45^\circ$), linearly polarized (-45°), right-hand circularly polarized and left-hand circularly polarized.

pair of parameters from cross-correlation function ρ, η we have in case $H_1 + H_2 = 1$ (S_0, S_1 remain unchanged):

$$S_2(\omega) = \frac{2\rho\,\sigma_1\sigma_2}{\pi}\,\frac{1-\cos(\omega)}{\omega^2}, \tag{20}$$

$$S_3(\omega) = -\eta\,\sigma_1\sigma_2\,\mathrm{sgn}(\omega)\,\frac{1-\cos(\omega)}{\omega^2}. \tag{21}$$

Notice that coherence function C_{ij} is here naturally involved and can be expressed by vector $\vec{S}$. Parameters $\vec{S}$ also give an insight into the statistical behavior of the process, Lefèvre et al. [20]. Important is also the degree of polarization[5] $0 \le p = \phi(\omega) \le 1$ (unpolarized when 0). It is closely related to the coherence[6] of the process (a measure of the coherency between its real and imaginary part). It might happen that two polarized processes with the same H have quite different magnitude of the ratio $\frac{\phi^e}{\phi^l} = \frac{S_3}{\sqrt{S_1^2+S_2^2}} = \frac{1}{\tan(2\chi)}$. This is a balance between linear and elliptical polarization, whereas a strong linear polarization is connected with the alignment of the process with a given direction. A strong elliptical polarization causes distinctive patterns made of intricated loops with a determined direction of rotation. Here we have to emphasize that polarization degree of a FGN less that 1 implies shaping an elliptical domain of admissibility for parameters ρ and η, see e.g. [2] for more details.

6. Analysis of a financial data

6.1. Real data

We apply the GTCLM model to a set of real data. The time series correspond to the trajectories to the value of the currencies in every second of the interval 18:31:00 - 19:02:00 hours (January 15, 2015) in the Japanese bank as illustrated on Fig. 7.

[5] I.e. the ratio of polarized energy over unpolarized energy - a measure of the shared power between the two marginal components of the process.

[6] Its square can be expressed as the sum of squares of the degree of linear polarization $\left(\phi^l = \frac{\sqrt{S_1^2+S_2^2}}{S_0}\right)$ and the degree of elliptical polarization $\left(\phi^e = \frac{S_3}{S_0}\right)$.

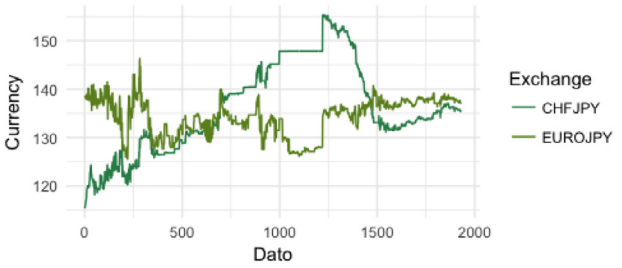

Fig. 7. Time series of the CHFJPY and the EUROJPY (every second during period 18:31:00–19:02:00, January 15, 2015 in the Japanese bank).

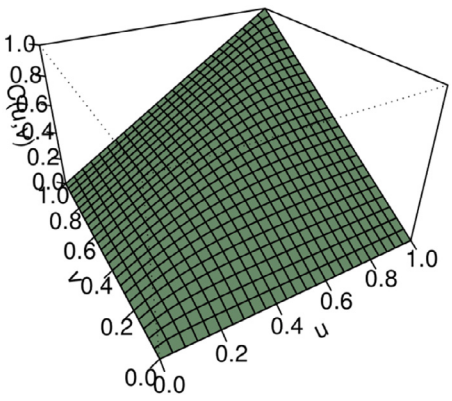

Fig. 8. Student t copula for bivariate modeling of pair currencies CHFJPY and EUROJPY (describes or models the dependence (inter-correlation) between them).

Table 1
$\hat{H}_1$ and $\hat{H}_2$ using discrete wavelet transform (for a real data).

Series	Regression line	$\hat{H}$
CHFJPY	$y = -0.7225j - 5.1073$	0.8613
EUROJPY	$y = -0.7578j + 4.5205$	0.8789

Initially we construct the 2-dimensional copula as illustrated on Fig. 8.

The density associated with the copula is observed on Fig. 3. With the copula and some measures associated with it, such as, $\rho = 0.756$ and $\lambda = 0.564$, we applying (7) with $r = 0.1138\pi$ and estimate $\hat{\nu}$ to obtain

$$\lambda = \frac{\int_{0.1138\pi}^{\frac{\pi}{2}} \cos^{\nu} t \, dt}{\int_{0}^{\frac{\pi}{2}} \cos^{\nu} t \, dt}. \tag{22}$$

We solve (22) and we obtain

$$\begin{aligned} 0 = &-0.564 + 2\Gamma\left(\tfrac{\nu}{2}+1\right)(0.94088^{(\nu+1)})\,{}_2F_1(1/2,(1+\nu)/2;(3+\nu)/2;0.88526) \\ &-\left(6.12323^2 \times 10^{(-17(1+\nu))}\right)\tfrac{{}_2F_1(1/2,(\nu+1)/2;(\nu+3)/2;3.74940\times 10^{(-33)})}{\sqrt{\pi}\,\Gamma((\nu+1)/2)(\nu+1)} \end{aligned} \tag{23}$$

The convergence of estimated degrees of freedom $\hat{\nu}$ is illustrated on Fig. 9.

Now, knowing that $\hat{\nu} \approx 4$, we proceed with the generation of the gamma distribution $W \sim Gamma(2, 2)$. Next, we determine its inverse and use (8) to construct the bivariate Gaussian distribution. Solving this allows us to extract the marginal Gaussian distributions for the CHFJPY and EUROJPY rates of currencies. For the analysis of the memory of each currency we verify the assumptions of stationary increments, self-similarity and dependence on the increments. Then we proceed with the estimation of the H parameter in each trajectory. We refer to the H parameter as an indicator of the memory of the process. We use the discrete wavelet transform method for Hurst exponent estimation. First we construct the regression lines for each of the currencies using the expression (14), and later, we estimate H parameter using (15). In particular, for the returns CHFJPY and EUROJPY we obtain the regression lines plotted on Figs. 10 and 11). The regression lines and the estimated values of $\hat{H}_1$ and $\hat{H}_2$ are provided in Table 1.

Recall that $\hat{H}$ parameter is associated with the fractal dimension and that it provides the degree of how rough the surface is for a set of self-similar increments. In particular, the bivariate stochastic process with $\hat{H}_1 = 0.8613$ and $\hat{H}_2 = 0.8789$ for the

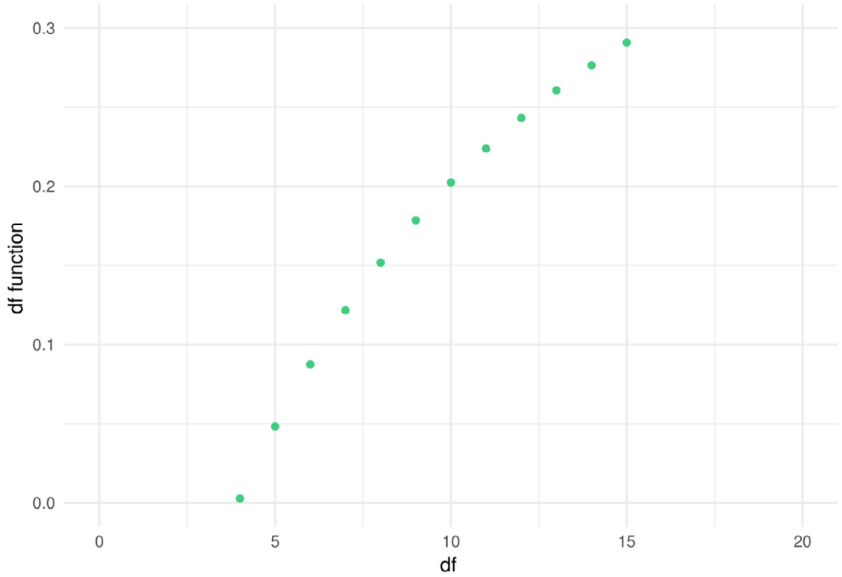

Fig. 9. Convergence of degrees of freedom $\hat{\nu}$ of the bivariate Student t copula given by the function in right hand side of Eq. (23).

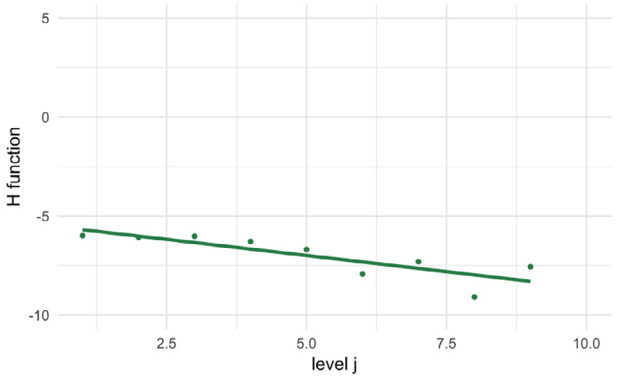

Fig. 10. CHFJPY regression line of decomposition level j from discrete wavelet transform vs. H function represented by expression (14).

two analyzed trajectories indicates that there are positive correlations between the series. The fractal curves are softer and the observations contain long-term dependence. In addition, values of $\hat{H}$ so close, guarantee that we are effectively focusing on the bivariate stochastic process associated with the joint behavior of currencies. From a practical point of view, the long-term memory for the series of financial returns on the CHFJPY and the EUROJPY indicates that there is a persistence, i.e., within certain periods of time, the value of the currency CHFJPY depends on the values in previous periods; in the same way it happens for the currency EUROJPY. With both components, i.e., the marginal behavior (memory of each of the trajectories) and the bivariate behavior ($\hat{\nu}$ of the bivariate Student t copula), we proceed with the reconstruction of the 2-dimensional stochastic process. We illustrate on Fig. 12 an approximation to the reconstructed stochastic process.

Finally, we expose the coherence function between the two FMBs according to the Eq. (19). When $p = 2$, for fixed values of H_1 and H_2, the condition $C_{12} \leq 1$ means that the set of possible parameters ρ_{12} and η_{12} is the interior of an ellipse. For the time series of the returns of the CHFJPY and EUROJPY with $\hat{H}_1 = 0.8613$ and $\hat{H}_2 = 0.8789$, we obtain the ellipse on Fig. 13. To be able to understand from a financial point of view the mechanism how the value of a certain currency measured in units of another currencies develops, we need to take a look on demand and supply curves. Although the outcome is the same the shifting of the curves differs depending from which country's point of view one sees it.

The equation on the ellipse is

$$\frac{\rho_{12}^2}{0.0012} + \frac{\eta_{12}^2}{0.00024} \leq 1. \tag{24}$$

Remember that the coherence function allows us to examine the relationship between two time series. In addition, for cases in which the assumptions of the linear system are insufficient, the Cauchy–Schwarz inequality guarantees that its value is less than 1, as is our case.

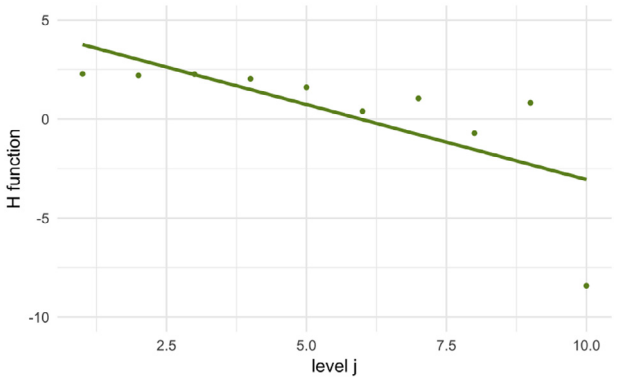

Fig. 11. EUROJPY regression line of decomposition level j from discrete wavelet transform vs. H function represented by expression (14).

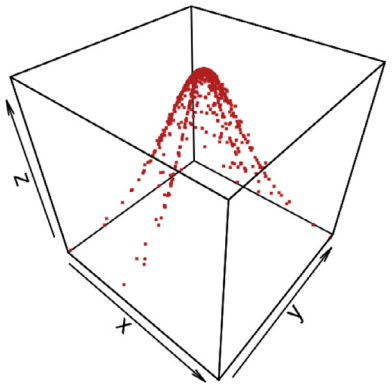

Fig. 12. Approximation of stochastic process reconstructed on real data using both components - marginal (Hurst exponents) and bivariate (ν, coherence) behavior.

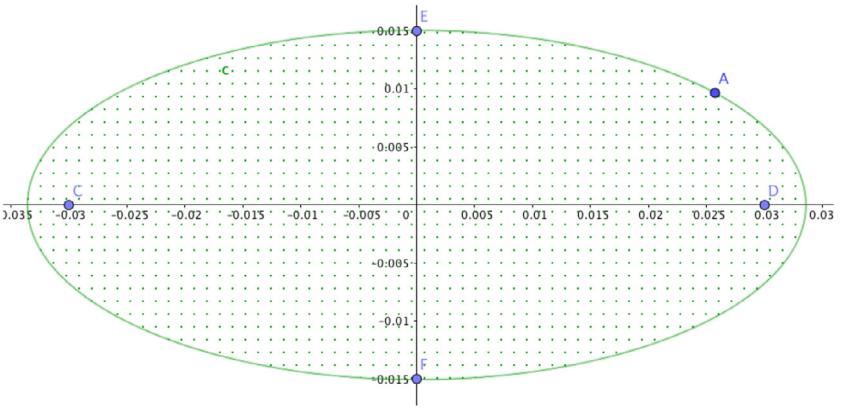

Fig. 13. Ellipse $C_{12}(\omega, \delta) \leq 1$ of the coherence function between the increments with $\hat{H_1} = 0.8613$ and $\hat{H_2} = 0.8789$. Notice that points A,B,C,D,E, F were reference points to create the graph in Geogebra.

6.2. Simulated data

Here we validate the GTCLM model on simulated data. We start by constructing Gaussian marginals, i.e., a FBM_1 and a FBM_2. The Hurst parameters simulated are $H_1 = 0.89$ and $H_2 = 0.87$. Additionally, $\boldsymbol{\mu}^1_{2000\times 1} = \mathbf{0}$, $\boldsymbol{\Sigma}^1_{2000\times 2000}$, $\boldsymbol{\mu}^2_{2000\times 1} = \mathbf{0}$ and $\boldsymbol{\Sigma}^2_{2000\times 2000}$. Remember that $\boldsymbol{\Sigma}$ is given by (see [3])

$$\text{Cov}(B_i^H, B_j^H) = \frac{1}{2}\left[\left(\frac{i}{n}\right)^{2H}\left(\frac{j}{n}\right)^{2H}\right] - \left|\frac{i}{n} - \frac{j}{n}\right|^{2H}. \tag{25}$$

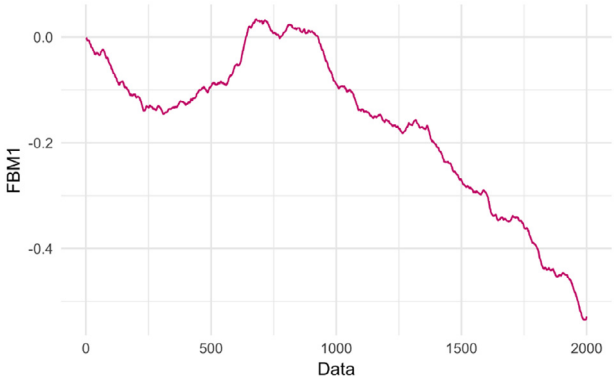

Fig. 14. Simulated trajectory of FBM_1 with $H_1 = 0.89$ and estimated covariance given by (25).

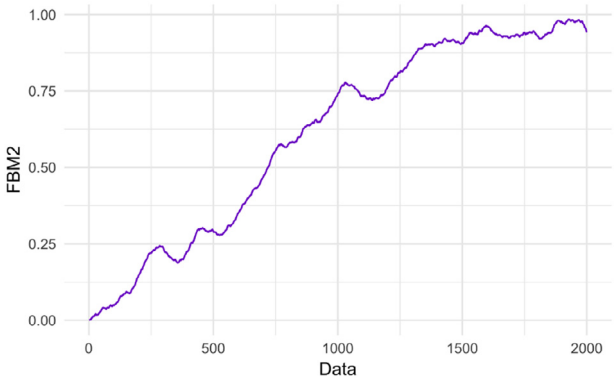

Fig. 15. Simulated trajectory of FBM_2 with $H_2 = 0.87$ and estimated covariance given by (25).

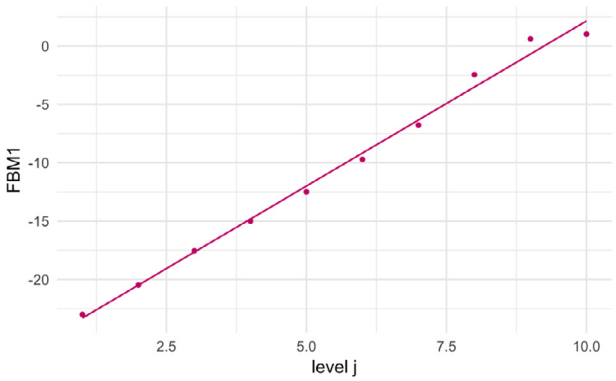

Fig. 16. Regression line for FBM_1 of decomposition level j from discrete wavelet transform vs. function represented by expression (14).

Fig. 14 illustrate the simulated FBM_1 and Fig. 15 the simulated FBM_2.

We use the discrete wavelet transform for estimate $\hat{H_1}$ y $\hat{H_2}$. Figs. 16 and 17 illustrate the regression lines according to (14).

The equations of the regression lines and the values of $\hat{H}$ can be seen on Table 2.

The equations on Table 2 indicate that both series contain long-memory. Additionally, the estimators have an mean square error close to zero. Finally, we expose the coherence function between the increments according to (19). For the simulated data $H_1 = 0.89$ and $H_2 = 0.87$, respectively, we get the ellipse on Fig. 18.

The equation on the ellipse is

$$\frac{\rho_{12}^2}{0.0011} + \frac{\eta_{12}^2}{0.00018} \leq 1. \tag{26}$$

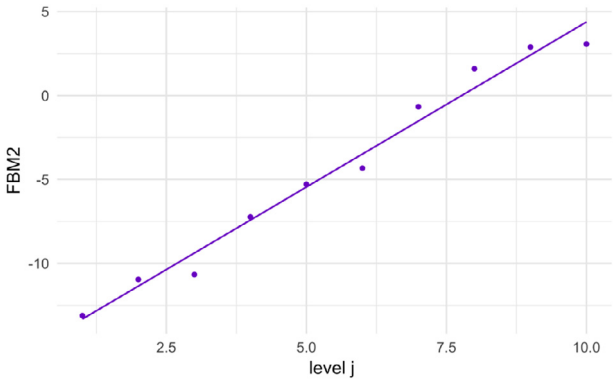

Fig. 17. Regression line for FBM_2 of decomposition level j from discrete wavelet transform vs. function represented by expression (14).

Table 2
$\hat{H_1}$ and $\hat{H_2}$ in FBM1 and FBM2, respectively.

Serie	Regression line	$\hat{H}$	H real
FBM1	$y = 2.74j - 26.135$	$\hat{H_1} = 0.87$	0.89
FBM2	$y = 2.68j - 15.284$	$\hat{H_2} = 0.84$	0.87

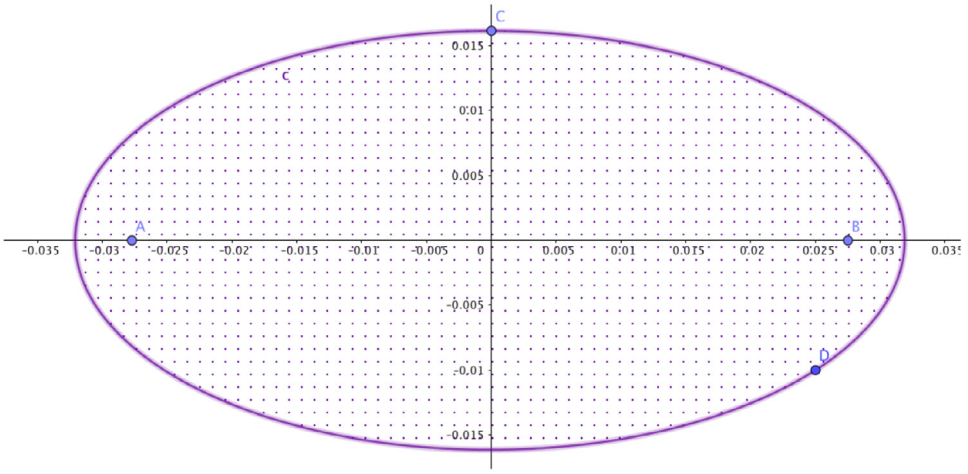

Fig. 18. Ellipse $C_{12}(\omega, \delta) \leq 1$ of the coherence function between the increments with $H_1 = 0.89$ and $H_2 = 0.87$. Notice that points A,B,C,D,E, F were reference points to create the graph in Geogebra.

It is important to clarify that for both simulated data and real data the nature of the stochastic process retains a dependence relationship between the variables. For real data the value of one currency affects the value of another; and for the simulated data, analogously.

7. Discussion

We can conclude that in finance the time series of returns do not always follow a Gaussian distribution. Frequently we can find returns that follow distributions with heavy tails, namely Student t. This was the case of the frequency for the returns of CHFJPY and EUROJPY currencies of the Japanese bank. We checked this fact by application of normality tests for each of the series. Additionally, the bivariate stochastic process that involves both currencies through the 2-dimensional copula illustrates the bivariate Student t copula as shown in Figs. 3 and 8. This justifies the empirically well observed fact that some bivariate time series of the FX market have heavy tails. We also found that it is possible to establish the link between a Gaussian and non-Gaussian process using copula functions and the transformation provided in Section 3. Calculating the tail dependence coefficients and constructing the 2-dimensional copula allowed us to analyze the convergence of the degrees of freedom for the bivariate stochastic process. That allows under regularity condition copula function to be a useful tool for the estimation of parameters associated with the trajectories of a stochastic process. In addition, we conclude that the use of transformation of a random variables (specifically the transformation of a random Student t variable into a

Gaussian) give us as a by-product the estimator of the degrees of freedom of the random Student t vector. We also conclude that the memory of the bivariate stochastic process becomes visible through the Hurst exponent H in each of its trajectories. That is, from the multivariate Gaussian distribution, we obtained the univariate marginals and later the value of H in each trajectory. Therefore, we highlight that the FX market series presents volatile and erratic behavior, and the description of the probabilistic model associated with them is complex and has its own characteristics in correspondence with the nature of the data. So the GTCLM model becomes an alternative for the construction and analysis of the probabilistic models on the FX market. Finally, we can conclude the prevalence of copulas of extreme values in the FX market. However, the time range analyzed determines the nature of the subjacent copula and the implicit stochastic process. Therefore, temporal variations become a determining factor in the analysis of a financial stochastic process. Our results can help to explain why the Purchasing Power Parity theory does not always hold. According to the Purchasing Power Parity theory the same amount of any currency could buy the same basket of products everywhere [9,22]. For example, with 100 USD it should be possible to buy the same amount of the same products in Switzerland or in Japan. That this is not always the case we can intuitive understand using The Economist's Big Max Index approach, comparing prices of the classic Mc Donald's hamburger in different countries. While in Japan it costs 3,6 USD, in Switzerland it costs 6,9 USD (Big Mac index - The Economist [7], see also [24,25]). In a future research, it would be interesting to explore the underlying reason for such violations in the stochastic process and the identified erratic behavior. Differences in market structures such as higher or lower degree of market concentration (monopolization) might play an important role here [10].

Acknowledgments

Partially supported by Fondecyt 1171335, Proyecto ANID/BASAL FB210005, Proyecto VOS, 22-MATH-08, MathAsmsud 19-06 and the Slovak Research and Development Agency under the contract no. APVV-16-0337 and APVV-17-0568. This work was also supported by grant VEGA MŠ SR 1/0526/20. We acknowledge support of the Editors and the informative and insightful suggestions of Referees

Supplementary material

Supplementary material associated with this article can be found, in the online version, at doi:10.1016/j.amc.2021.126871

References

[1] P. Abry, P. Flandrin, M. Taqqu, D. Veitch, Self-similarity and long-range dependence through the wavelet lens, Theory Appl. Long-Range Depend. (2000) 1–25.
[2] P.-O. Amblard, J.-F. Coeurjolly, F. Lavancier, A. Philippe, Basic properties of the multivariate fractional Brownian motion, in: Self-Similar Processes and Their Applications. Selected Papers Related to the Conference, Angers, France, July 20–24, 2009, Société Mathématique de France, Paris, 2013, pp. 63–84.
[3] C. Bahamonde, Comparación de Metodologías Para Estimar el Parámetro de Hurst en un Modelo con Larga Memoria, Pontificia Universidad Católica de Valparaíso, Valparaíso, 2014. Advisor: Soledad Torres
[4] N. Balakrishnan, C. Lai, Continuous Bivariate Distributions, Springer New York, 2009. https://books.google.at/books?id=bxHmvSziRWwC
[5] A. Bárdossy, J. Li, Geostatistical interpolation using copulas, Water Resour. Res. 44 (7) (2008) 1–15.
[6] H.Y.D. Sigaki, P. Matja, H.V. Ribeiro, Clustering patterns in efficiency and the coming-of-age of the cryptocurrency market, Sci. Rep. 1440 (2019), doi:10.1038/s41598-018-37773-3.
[7] M.R. Datastream, "The Economist - The Big Mac Index", 2020, https://www.economist.com/big-mac-index.
[8] S. Demarta, A. J. McNeil, The t Copula and Related Copulas, Federal Institute of Technology ETH Zentrum, 2004.
[9] R. Dornbusch, S. Fischer, R. Startz, Macroeconomia, eleventh edition, Bookman Editora, 2013. https://books.google.sk/books?id=MB44AgAAQBAJ
[10] F. Fuders, N. Michaelis, et al., Marktkonzentration: ein großes hindernis für eine nachhaltige ökonomie, in: H. Rogall, et al. (Eds.), Jahrbuch Nachhaltige Ökonomie 2016/2017, Metropolis, Marburg, 2016, pp. 271–294.
[11] E. Ortega, Ch. Osbat, Exchange rate pass-through in the euro area and EU countries, in: E. Ortega, Ch. Osbat (Eds.), Occasional Paper Series ECB Frankfurt 2020, vol. 241, ECB, Frankfurt, 2020.
[12] M. Hans, Estimation and Model Selection of Copulas with an Application to Exchange Rates, Research Memorandum, Maastricht University, Maastricht Research School of Economics of Technology and Organization (METEOR), 2007. https://EconPapers.repec.org/RePEc:unm:umamet:2007056
[13] M. Hornbrook, "Was David Li the guy who 'blew up Wall Street?", 2009, https://www.cbc.ca/news/canada/was-david-li-the-guy-who-blew-up-wall-street-1.775732.
[14] H. Hult, F. Lindskog, Multivariate extremes, aggregation and dependence in elliptical distributions, Adv. Appl. Probab. 34 (3) (2002) 587–608, doi:10.1239/aap/1033662167.
[15] C.L. Jones, G.T. Lonergan, D. Mainwaring, Wavelet packet computation of the hurst exponent, J. Phys. A 29 (10) (1996) 2509.
[16] I. Kaplan, Estimating the Hurst Exponent, Independent Software Consultant and Founder, Dutch Caribbean, 2013.
[17] C. Kelly, "Meet the man whose big idea felled Wall Street.", 2009, https://www.thestar.com/business/2009/03/18/meet_the_man_whose_big_idea_felled_wall_street.html.
[18] L. Kirichenko, T. Radivilova, Z. Deineko, Comparative analysis for estimating of the hurst exponent for stationary and nonstationary time series, Inf. Technol. Knowl. 5 (1) (2011) 371–388.
[19] F. Lavancier, A. Philippe, D. Surgailis, A two-sample test for comparison of long memory parameters, J. Multivar. Anal. 101 (9) (2010) 2118–2136, doi:10.1016/j.jmva.2010.04.003.
[20] J. Lefèvre, N. Le Bihan, P. Amblard, A geometrical study of the bivariate fractional gaussian noise, in: 2018 IEEE Statistical Signal Processing Workshop (SSP), 2018, pp. 144–148, doi:10.1109/SSP.2018.8450737.
[21] D.X. Li, On default correlation: a copula function approach, J. Fixed Income 9 (4) (2000) 43–54.
[22] G. Mankiw, M. Taylor, Economics 3, Cengage Learning EMEA, 2014. https://books.google.sk/books?id=-EuCnQAACAAJ
[23] R. Nelsen, An Introduction to Copulas, Springer Series in Statistics, 2006, doi:10.1007/978-0-387-98135-2.
[24] T.J. O'Brien, S. Ruiz de Vargas, Currency indexes and consistent currency misvaluation: illustrations using Big Mac data, Res. Int. Bus. Finance 48 (2019) 464–474, doi:10.1016/j.ribaf.2018.09.012.
[25] C. Rabe, A. Waddle, The evolution of purchasing power parity, J. Int. Money Finance 109 (2020) 102237, doi:10.1016/j.jimonfin.2020.102237.

[26] M. Rosenblatt, Remarks on a multivariate transformation, Ann. Math. Stat. 23 (3) (1952) 470–472, doi:10.1214/aoms/1177729394.
[27] M.Á. Sánchez Ovando, Estimación de Parámetros y Pronósticos en Modelos Tar con Errores t-student, Centro de Investigación en Matemáticas, A.C., De Jalisco s/n, Valenciana, 36023 Guanajuato, Gto., México, 2015.
[28] C. Scheffler, A derivation of the em updates for finding the maximum likelihood parameter estimates of the student's *t* distribution, Technical note. URL http://www.inference.phy.cam.ac.uk/cs482/publications/scheffler2008derivation.pdf (2008).
[29] D. She, A.K. Mishra, J. Xia, L. Zhang, X. Zhang, Wet and dry spell analysis using copulas, Int. J. Climatol. 36 (1) (2016) 476–491.
[30] G. Shevchenko, Fractional Brownian motion in a nutshell, Int. J. Mod. Phys. 36 (2015) 1560002, doi:10.1142/S2010194515600022.
[31] A. Sklar, Fonctions de répartition án dimensions et leurs marges, Publ. Inst. Stat. Univ. Paris 8 (8) (1959) 229–231.
[32] J. Villa, Movimiento browniano fraccionario, Morfismos 2 (1) (1998) 47–65.
[33] S. Wang, S. He, A. Yousefpour, H. Jahanshahi, R. Repnik, M. Perc, Chaos and complexity in a fractional-order financial system with time delays, Chaos Solitons Fractals 131 (2020) 109521, doi:10.1016/j.chaos.2019.109521.
[34] J. Xu, J. Ma, M.H. Connors, H. Brodaty, Proportional hazard model estimation under dependent censoring using copulas and penalized likelihood, Stat. Med. 37 (14) (2018) 2238–2251.